JCTC Journal of Chemical Theory and Computation

Article

pubs.acs.org/JCTC

The Silica–Water Interface: How the Silanols Determine the Surface Acidity and Modulate the Water Properties

Marialore Sulpizi,[†] Marie-Pierre Gaigeot,*[,‡,§] and Michiel Sprik[∥]

[†]Johannes Gutenberg University, Staudinger Weg.7, D 55099, Mainz, Germany

[‡]LAMBE UMR8587, Université d'Evry val d'Essonne, Blvd F. Mitterrand, Bat Maupertuis, 91025 Evry, France

[§]Institut Universitaire de France (IUF), 103 Blvd St Michel, 75005 Paris, France

[∥]Department of Chemistry, University of Cambridge, Cambridge CB2 1EW, United Kingdom

Supporting Information

ABSTRACT: Silica is the most abundant metal oxide and the main component of the Earth's crust. Its behavior in contact with water plays a critical role in a variety of geochemical and environmental processes. Despite its key role, the details of the aqueous silica interface at the microscopic molecular level are still elusive. Here we provide such a detailed understanding of the molecular behavior of the silica–water interface, using density functional theory based molecular dynamics (DFTMD) simulations, where a consistent treatment of the electronic structure of solvent and surface is provided. We have calculated the acidity of the silanol groups at the interface directly from the DFTMD simulations, without any fitting of parameters to the experimental data. We find two types of silanol groups at the surface of quartz: out-of-plane silanols with a strong acidic character (pK_a = 5.6), which consequently results in the formation of strong and short hydrogen bonds with water molecules at the interface, and in-plane silanols with a pK_a of 8.5, forming weak hydrogen bonds with the interfacial water molecules. Our estimate of the quartz point of zero charge (1.0) is found in good agreement with the experimental value of 1.9. We have also shown how the silanols orientation and their hydrogen bond properties are responsible for an amphoteric behavior of the surface. A detailed analysis has identified two species of adsorbed water molecules at the solid–liquid interface, which using the language of vibrational spectroscopy can be identified as "liquid-like" and "ice-like" water or, in other words, water molecules forming respectively weak and strong H-bonds with the oxide surface. These two populations of water are in turn responsible for two distinct peaks in the infrared spectrum of interfacial water and thus provide a molecular explanation of the experimental sum frequency generation spectrum recorded in the literature. In the specific case of quartz, we show that the liquid-/ice-like behavior is the result of the silanol groups ability to donate or accept hydrogen bonds with different strengths, which consequently modulates the vibrational properties of the adsorbed water layer.

INTRODUCTION

Surface science and interfacial chemistry are emerging fields where the detailed knowledge of the structure and electronic properties of surfaces of complex materials and the interactions of these surfaces with their surroundings is mandatory.[1−6] Complex phenomena arise at solid–liquid interfaces, leading to surface induced changes that are not only important for the solid but also for the liquid. In that respect, water plays an important role in a number of interfacial phenomena encountered in biological, chemical, and physical processes.[7,8] Water in contact with a solid can differ substantially from bulk liquid water,[9] even with an inert surface like gold,[10] and interactions with metal oxide surfaces in particular are very likely to disrupt the hydrogen-bonding network as it exits in the bulk liquid. Such water–oxide interfaces play a key role in environmental and geochemical processes[11−14] where they are, for instance, responsible for many catalytic reactions in solution and are believed to have played a central role in early prebiotic chemistry.[15] The chemical behavior of the oxide surface typically controls dissolution/precipitation, sorption, and redox and adsorption reactions.[5,14]

Among solid oxides, silica plays a special role as the most abundant solid compound in the earth crust and the main constituent of nanotechnological devices. Numerous technological applications of silica rely on its specific surface properties, and the surface silanol groups serve as hydrogen-bonding sites for a variety of chemical species, their reactivity enabling convenient chemical modifications which makes silica surfaces strategic for instance in biosensing applications.[16,17]

Surface acidity plays a central role in the chemical processes occurring at the interface. Experimentally, surface acidity is manifested in a net surface charge changing over from positive to negative with increasing pH. Because of the inherent difficulty for titration measurements to distinguish between the contributions of various functional groups, modeling of surface acidity has always played an important role in the understanding of relevant quantities, such as the pH at the point of zero charge (PZC). An approach commonly encountered in the literature is to parametrize empirical models for surface acidity using the pK_a values of solution monomers, which are chemically better characterized and more easily measured. The most successful and popular of these methods, the modified MUSIC model[18] uses bond valence to predict pK_a values, as does the

Received: October 10, 2011
Published: February 6, 2012

   dx.doi.org/10.1021/ct2007154 | J. Chem. Theory Comput. 2012, 8, 1037−1047

method of Bickmore et al.[19] The appeal of bond valence methods for pK_a prediction is the use of structural information, which is translated in prediction of chemical behavior. Bond lengths of relaxed structures determined by diffraction experiments or ab initio structure optimizations can be used to refine the bond valence methods.[20] A similar approach underlies the single site solvation bond strength and electrostatic (SBE) model.[21,22] The SBE model is based on a thermodynamic dielectric continuum approach, whereas the modified MUSIC model depends on explicit hydration, analogously to an implicit continuum solvation versus explicit solvent descriptions for liquid phase modeling. The advantages and disadvantages of both models have been discussed, e.g., in ref 23.

Even if silica could appear as one of the simplest cases of oxides, it seriously challenged the applicability of these models, thus requiring improvements with respect to the original versions. Indeed, the original MUSIC formulation in ref 24 could not account for quartz acidity. That model relies on the correlation between the pK_a values of surface functional groups with those of the analogous groups in solution monomers.[25] However that is not the case for silica which appears to be an outlier in such correlation relations.[21,22,25] This is compensated in the revised MUSIC model[18] by increasing the coordination number of silanols. Hence, the new predicted surface acidity reconciles with experiments if an exposed silanol group is assumed with an overall coordination number of three. The apparent contradiction is explained by the SBE model as the result of the low dielectric constant of quartz which enhances the difference between acidity of surface groups and solvated monomers. However, if the SBE model explains silica behavior with the same model used for other oxides, then it cannot actually provide any insights in terms of solvent structure at the surface, by construction.

Furthermore, differentiating between specific surface site geometries can be difficult for empirical models which normally use one or two generic sites with equilibrium constants and fitted density of sites. This limits the insight into molecular scale surface processes provided by this approach. One of the critical issues here is an adequate treatment of solvent effects. The effect of solvation has been a central theme in the development of computational methods for the study of physical and biological systems. The progress that has been made is impressive. Hence, state of the art self-consistent solvent reaction field methods can achieve an accuracy of ≈0.5 of a pK_a unit in the prediction of pK_a of molecules in solution.[26,27] However, in the case of strong and specific interactions of solvent molecules with the solute, the accuracy of these methods can be questionable. A proper description of solvent accessibility and coordination of the different functional groups may require an explicit molecular treatment of the solvent. Acid or basic sites on oxide surfaces with their highly heterogeneous environment are likely to fall into this category.

In DFT-based molecular dynamics simulations (DFTMD) simulations, the solute (oxide surface in the present interfacial context) and the solvent (electrolyte solution) are treated at the same level of theory, which includes the full electronic structure in a consistent way. Indeed the adsorbed water layer forms explicit molecular interaction with both the surface and the bulk water. This sets the motivation and technical context of the present paper in which we extend a recently developed all-atom density functional method for the calculation of molecular acidity to the calculation of the acidity of an oxide surface.[28−33]

Our system of interest is the hydroxilated (0001) α-quartz surface. The molecular configurations and wetting properties of water at the interface of silicon oxide surfaces have already been investigated in a number of classical force field-based simulations[34−36] and electronic structure calculations using DFT.[36−42] Here we address two new aspects, where DFTMD prove an accurate and pivotal method to predict properties from first principles and provide a microscopic interpretation of experimental data.

We address the calculation of the PZC of quartz from the acidity of surface groups. The microscopic origin of the surface acidity is discussed and the corresponding equilibrium constants are computed. Properties of the confined water between two silica layers are also investigated. In particular we calculate the dissociation constant of water in the confined environment. Anticipating our results, we can say that within our accuracy the water dissociation constant in the confined layers is the same as that in bulk water.

We furthermore analyze the water structure at the quartz interface, and we give an interpretation of recent spectroscopy experiments. In the last years sum frequency generation (SFG) spectroscopy, a second-order nonlinear optical technique has permitted to selectively investigate properties of interfaces. Shen has been one of the pioneers of this technique,[43−48] measuring in particular the SFG spectrum of the α-quartz (0001)−water interface. SFG experiments on the neutral (low pH) quartz−water hydrophilic interface give two bands, respectively located at ∼3200 and ∼3400 cm^{-1} .[44,47,49,50] It is striking that the 3200 cm^{-1} band occurs at the same frequency as in IR and Raman of ice,[51,52] while the 3400 cm^{-1} band is approximately found at the same frequency as in the infrared (IR) and Raman of liquid water.[53−55] Note that the 3200 cm^{-1} band is gaining in intensity at higher pH. Assignment of these two SFG peaks is still debated,[4]with two prevailing views in the literature: (1) The peak at 3200 cm^{-1} arises from a H-bond network of water molecules with an "ice-like" ordering, representative of O−H stretch of water molecules tetrahedrally coordinated, while the peak at 3400 cm^{-1} comes from a "liquid-like" arrangement of the water molecules, i.e., more disordered H-bond network.[44,47,49] These statements still need to be rationalized in terms of local molecular arrangements, as ice- and liquid-like do not signify that ice and liquid water are coexisting at the interface. At high pH, because the quartz surface becomes deprotonated and thus negatively charged, the surface field will induce more ordering in the hydrogen bond (H-bond) network at the interfacial region, thus amplifying the ice-like peak in the vibrational spectrum. At low pH, the surface is neutral and composed of silanol groups. One would thus expect that the orientation of the water molecules at the solid interface depends on the H-bonds formed with the silanol groups. Vibrational sum frequency generation (VSFG) phase measurements by Shen et al.[49] indeed support opposite polar orientation of the interfacial water molecules at low- and high-pH. (2) Another interpretation is that contributions to the 3400 cm^{-1} band mainly arises from water molecules directly adjacent to the surface, while the 3200 cm^{-1} peak comes from water molecules in the following water layers.[50] Namely, it means that water molecules immediately adjacent to the hydrophilic interface would form fewer H-bonds[50,56] and would be the major contributor to the 3400 cm^{-1} signal. Any subsequent layers that still do not display the isotropic characteristics of bulk water (thus still SFG active) will have tetrahedral bonding and then will contribute to the 3200 cm^{-1} signal.

Note that the surface electric field can polarize and orient several layers of water molecules into the bulk phase, and thus the near interface region also contributes to the SFG nonlinear signal,[57] though to what extent (i.e., how many layers) is not clear.

From the present microscopic DFTMD simulations, the vibrational IR active signatures of the quartz−water interface have been characterized, shedding new lights into these interpretations. The strength of our work is that all water molecules and all groups of the quartz bulk surface are individually represented at the same ab initio level, and their contribution to the final spectra have been individually quantified. We analyze the details of the water structure at the interface and unravel the origin of the two ice- and liquid-like behaviors from the first adsorbed layers. These behaviors are rationalized in terms of different types of H-bond and different H-bond strengths between water molecules and silanol groups, in direct relation with the calculated acidity constants of the surface silanol groups accessible for H-bondings at the interface.

RESULTS AND DISCUSSION

Water at the Interface: Structure and Spectroscopy. A snapshot of the hydroxilated (0001) α-quartz−water interface simulated in the present work can be found in Figure 1. Due to periodic boundary conditions applied in the modeling, the bulk liquid water is confined between two replicas of the quartz surface. Such issue is discussed later on in the paper, where we show that it has no influence on the final conclusions. The first result from our simulations is that water is strongly adsorbed on the (0001) quartz surface, as shown by the atomic probability density profile normal to the interface, which is given in Figure 2. In both the oxygen (red line) and hydrogen (black line) density profiles, there is one pronounced maximum close to each surface, which we identify with the adsorbed layer of water. The density distribution is, to a good approximation, symmetric with respect to the center of the water layer, with a slight asymmetry to be attributed to the limited duration of the simulation run and to the limited sample size.

The two surfaces in the sample remain fully hydroxilated over the entire trajectory. A rearrangement in the H-bond network with respect to the dry surface has quickly been established as a result from the competition of the H-bonds formed between hydroxyl−water and hydroxyl−hydroxyl groups. We find that only half of the silanol−silanol in-plane H-bonds that existed in the dry surface are maintained when the surface is wetted, namely the ones which are the shorter in the dry surface (see Figure 3). Calculating the angle formed by the silanol OH vectors with the direction normal to the interface, we find that the distribution of angles is bimodal, with two peaks, respectively, located at ∼20° and 102°. The first peak of the distribution corresponds to (Si)O−H groups pointing out-of-the plane of the surface toward the liquid water, while the second peak corresponds to silanol groups located in the plane of the surface. In plane and out of plane silanols alternate to form intrasurface H-bonds. The in-plane silanol−silanol O···H distance is 1.73 Å, as calculated from the first peak position in the O···H radial distribution function (black line in Figure 4) and is very close to the value for the optimized dry surface (1.74 Å).[39] These in-plane silanols also accept one H-bond from a nearby water molecule, as shown by the peak located at 1.82 Å in the radial distribution function (rdf) between the surface oxygens and water hydrogens (red line in Figure 4). The other half of the silanols stick out of the plane of the surface once wetted, and they consequently donate a strong and a short H-bond to a nearby water molecule, as revealed by the peak located at 1.64 Å in the rdf between the surface hydrogens and water oxygens (blue line in Figure 4). The alternate organization of water H-bond donors and acceptors in the interfacial layer above the quartz solid is schematically presented on the right-hand side of Figure 4.

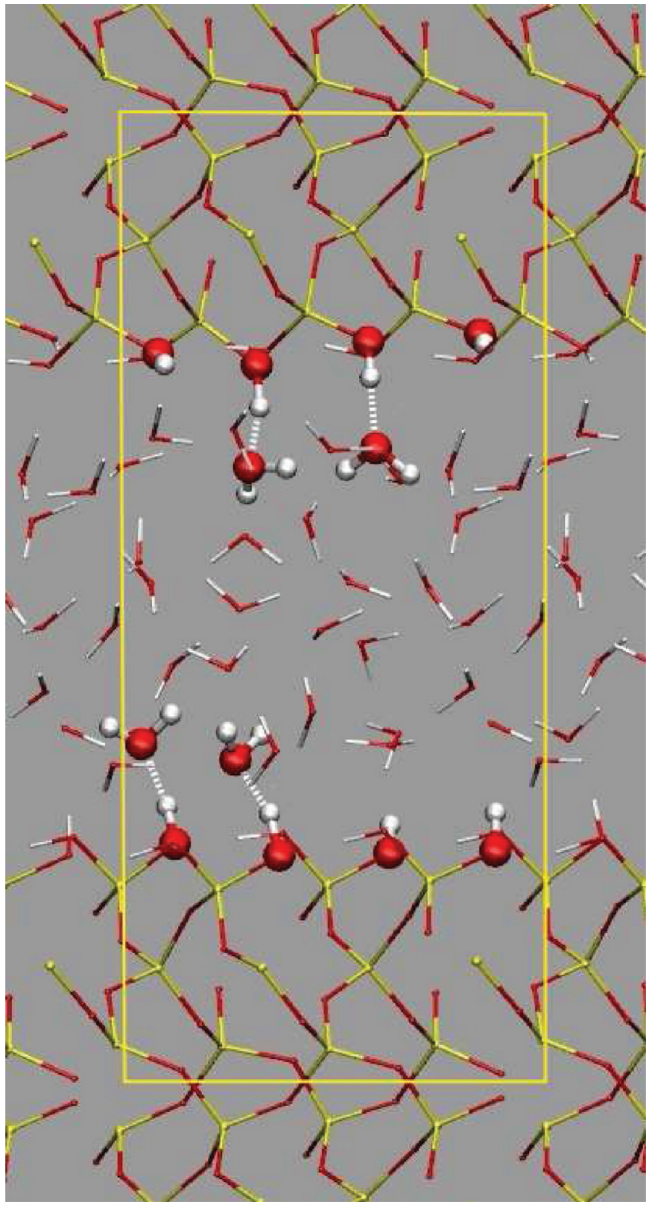

Figure 1. The (0001) α-quartz−water interface system from a snapshot of the simulation (xz side view, the unit cell in the x and z directions is marked with a yellow line). The three-dimensional periodic simulation cell contains 6 O−Si−O layers, with two fully hydroxilated surfaces (in total 24 Si, 56 oxygen, and 16 hydrogen atoms) and 32 water molecules. In this picture the silanol groups donating a H-bond to the solvent molecules are hilighted with ball and stick rendering.

This amphoteric behavior of the surface silanols is consistent with what was found by Yang and Wang[39] in a computational study where they placed one or two individual water molecules on a (0001) α-quartz surface and with previous DFT-based MD simulations.[36,41,42] Here we furthermore quantify the water orientation at the surface. This is done by defining a unit vector

dx.doi.org/10.1021/ct2007154 | J. Chem. Theory Comput. 2012, 8, 1037−1047

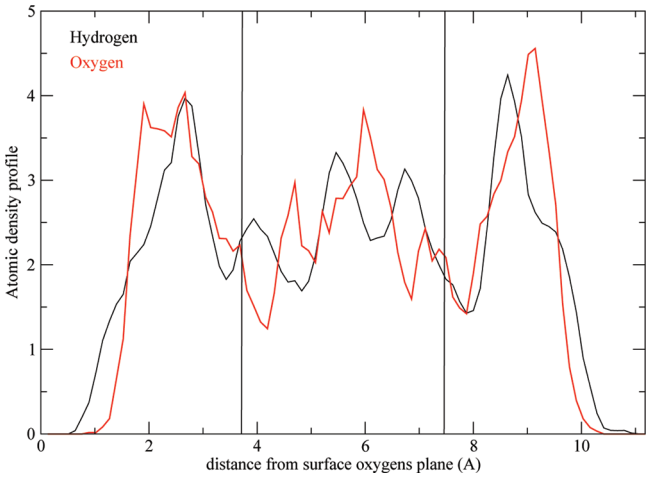

Figure 2. Atom density profile through the water layers. The zero is placed in the plane defined by the oxygens on the surface. The profile for the water oxygens and hydrogens are, respectively, in red and black.

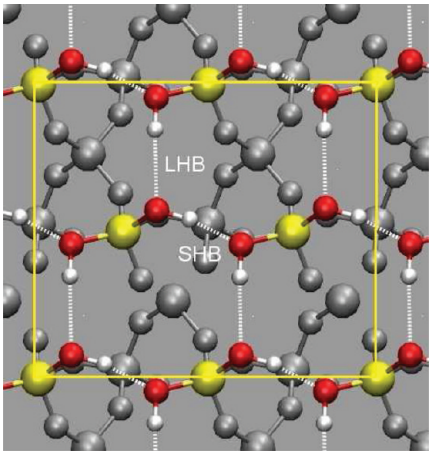

Figure 3. Dry hydroxilated α-quartz surface (xy plane). The surface silanol groups are highlighted in color: Si, yellow; O, red; and H, white. The H-bonds between nearby silanols are marked with a dashed white line. There are short H-bonds (SHB, distance 1.75 Å) and long H-bonds (LHB, 2.35 Å). The unit cell in the x and y directions is materialized with the yellow line.

in the atomic plane of the H_2O molecules bisecting the two OH bonds and calculating the average angle formed by this vector with the quartz surface xy plane. The projection normalized to the number of water per layer is given in Figure 5 (averaged over the two surfaces of our sample, but equivalent structures are found for both surfaces). We observe that the adsorbed waters tend to be oriented with their dipole moment parallel to the surface plane (angle of 25−30°). As a guideline, the value for an isotropic distribution ($\pi/4$ = 0.785, angle of 38°) is also reported in Figure 5 (black line), showing that the subsequent layers of bulk liquid grossly display such an isotropic orientational order, on average. A recent investigation of the fused silica−water interface[12] has shown a comparable orientation of the adsorbed water molecules, even though caution should be taken in this comparison as the glassy fused surface is not structurally as organized as the neutral quartz surface investigated here, which should alter the comparisons. As anticipated, the orientation of water molecules in the first adsorbed layer can be separated in two families, depending whether water accepts or donates a H-bond with the surface. The dipole

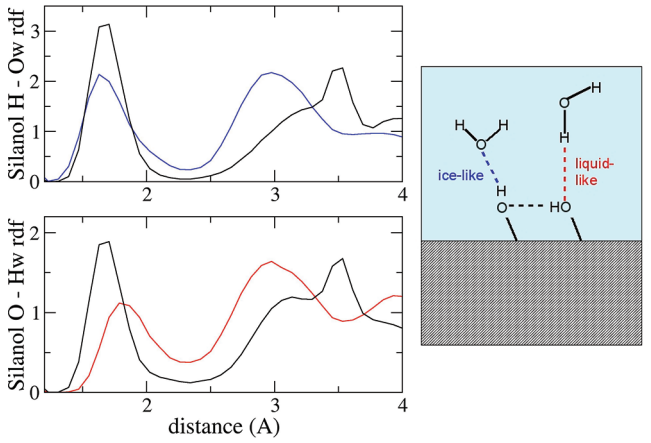

Figure 4. Radial distribution function for the surface silanol hydrogen atoms and the oxygen atoms of the water solvent (O_w) at the top (blue line), and rdf for the silanol surface oxygens atoms and the hydrogen atoms of the water solvent (H_w) at the bottom (red line). Top and bottom: For comparison, the black line reports the rdf between oxygen and hydrogen atoms of the in-plane silanols forming in-plane H-bonds.

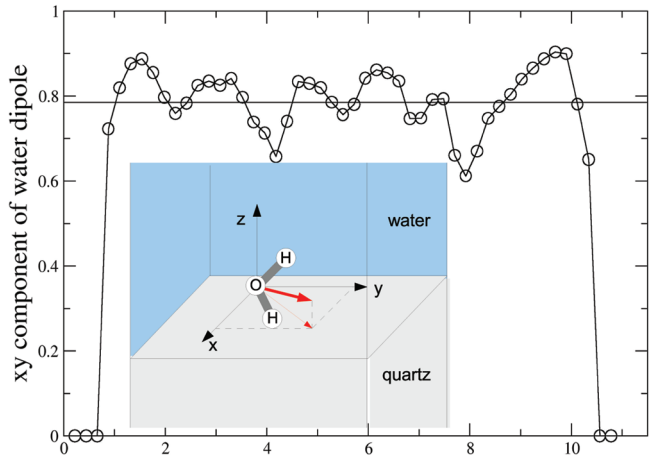

Figure 5. Water orientation at the quartz interface as function of the distance from the interface along the z direction perpendicular to the surface. See text for the details of the calculation, but a pictorial description of the unit vector (thick red arrow) and its projection in the xy plane of the surface (thin red arrow) are presented in the inset.

orientation for the two subfamilies is indeed different. The acceptors have a dipole which points away from the surface and form an angle of about 30−60° with the z axis. The donors dipole, on the other hand, points toward the surface forming and angle of about 120−150° with the z axis (see also Figure 6).

Vibrational spectroscopy is a powerful and precise probe for the structure and dynamics of materials. SFG experiments in particular provide such a selective approach to interfaces, and the recent advances in nonlinear optical technology have propelled a new era for surface spectroscopy.[58] SFG experiments from Shen's group and others[44,47,49,50] on the neutral (low pH) quartz−water interface give two bands respectively located at ∼3200 and ∼3400 cm^{-1}. As mentioned before, such features are reminiscent of both liquid- and ice-like water,[4,44,47,49,58,59] or put into the language of spectroscopists, such features are respectively characteristic of weak and strong H-bonds formed between the surface and the liquid water. This has been observed not only for silica but also for other materials, such as alumina,[48] and has raised debates on its

dx.doi.org/10.1021/ct2007154 | J. Chem. Theory Comput. 2012, 8, 1037−1047

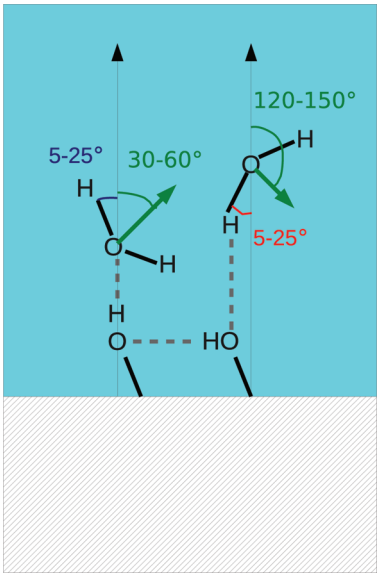

Figure 6. Schematic illustrations of the orientations of water molecules in the interfacial region of quartz, with respect to the z axis normal to the surface (vertical black arrows). Left side: a water which is accepting a H-bond from the surface out-of-plane silanol. Right side: a water molecule which is donating a H-bond to the surface in-plane silanol. The green arrow reports the dipole moment of the water molecules.

significance at the molecular level, in particular trying to relate the peaks with the water molecules that contribute to them in terms of distance (layers) above the surface, coordination, or orientation. Our aim here is to provide a microscopic molecular interpretation of these spectroscopic features.

Hereafter, the interfacial water molecules are defined as forming direct H-bonds with the quartz surface (first adsorbed layer), while the rest of the water molecules constitute the bulk liquid in the subsequent layers above the surface. We find that the interfacial water molecules as well as the bulk liquid water molecules are on average tetrahedrally coordinated. The interfacial waters form an average total of 4.3 H-bonds, roughly decomposed into 3.0 H-bonds with water and 1.0 H-bonds with the surface silanols, while the bulk waters form on average 3.8 H-bonds (as in pure liquid water, with the same theoretical setup). In particular, the interfacial waters do not appear to be under-coordinated with respect to the bulk layers, contrary to what can be sometimes assumed in literature.[4,57] The most striking feature of particular interest here is that two 'species' of interfacial water molecules can be distinguished according to which silanol sites they are bound to: This consequently modulates both their internal bond lengths and the strength of their H-bond network, as we will demonstrate now. Results are schematically illustrated in Figure 6.

We find that the water molecules which donate a H-bond to the in-plane surface silanols have $H_w\cdots O_{Si}$ H-bonds of 1.82 Å, similar to the $H_w\cdots O_w$ of 1.81 Å of pure liquid water (with the same theoretical setup) and an internal O_w-H_w covalent bond of 0.988 Å, very close to the 0.990 Å of pure liquid water. The water molecules which accept a H-bond from the out-of-plane silanols have a very short $O_w\cdots H_{O-Si}$ H-bond of 1.64 Å which is similar (still shorter) to the short $O_w\cdots H_w$ of 1.76 Å of ice. Consequently, they display long O_w-H_w covalent bond lengths with a mean value of 0.996 Å, which is very close to the 0.999 Å value obtained in ice.

We can thus identify two types of interfacial water molecules H-bonded to the quartz surface: one type that we can call liquid-like water and one type ice-like (for a visual sketch see Figures 4 and 6) because of their respective covalent O_w-H_w and H-bond lengths properties. To go one step further, we show below that these two species give rise to two distinct peaks in the IR spectrum of the interfacial water, in agreement with the notion of liquid- or ice-like vibrational features used in the literature of SFG spectroscopy. SFG is second-order nonlinear optical technique. Its intensity includes both dipole and polarizability derivatives,[44,47,49,58,60] thus probing molecules which are both IR and Raman active. It thus appears reasonable, in a first approximation, to anticipate SFG features in the vicinity of IR and/or Raman maxima. Here we use the IR signatures computed from our DFTMD simulations to investigate the 3000−4000 cm^{-1} domain, which is particularly sensitive to the density and the structure of the H-bond network at the water−solid interface.

The IR spectra of the surface silanols and liquid water (following the separation through different layers above the surface) are presented in Figure 7. IR spectra of ice and pure

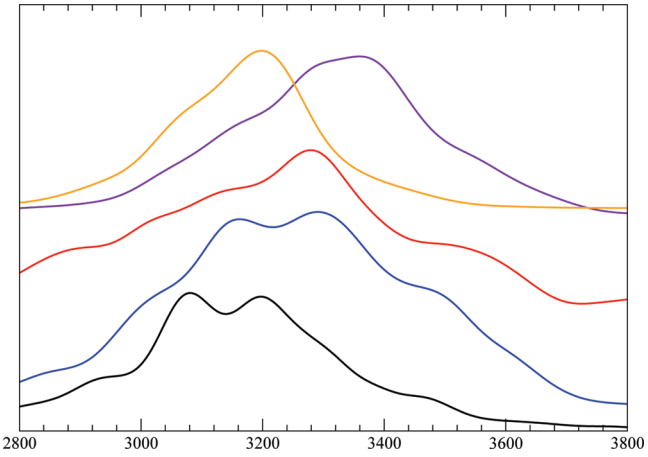

Figure 7. Vibrational IR spectra calculated through the present investigation. Bottom to top: IR spectra of silanols (black), water adsorbed at the surface (blue), subsequent layers of water molecules (red), pure liquid water (violet), and pure ice (orange). The IR spectra are given as products $\alpha(\omega)n(\omega)$ expressed in cm^{-1} as a function of reciprocal wavenumber ω in cm^{-1}.

liquid water can also be found in this figure and are used as references for discussion (again, these results have been obtained as the same level of theory as the interface simulation). The velocity density of states (VDOS) decompositions discussed hereafter can be found in Figure 2 of the Supporting Information (ref 61 covers the detailed analyses and properties of VDOS; note only here that VDOS provide all vibrational signatures, i.e., IR active and nonactive). We find that the IR spectrum of the interfacial water molecules which are directly H-bonded to the quartz surface (blue line) is composed of two main peaks located at ∼3160 and ∼3300 cm^{-1}. Shoulders can also be distinguished at ∼3480 and ∼3000 cm^{-1}. SiOH silanols at the surface (black line) also give rise to two IR bands in the same domains, at ∼3080 and ∼3200 cm^{-1}, red-shifted from the two interfacial water bands by ∼100 cm^{-1}. The presence of peaks for silanols and interfacial water in a common range, though shifted by 100 cm^{-1}, is enough to enable vibrational couplings between silanols and H-bonded waters, thus giving rise to the interfacial SFG signals recorded in the literature. The two subsequent layers of water molecules

dx.doi.org/10.1021/ct2007154 | J. Chem. Theory Comput. 2012, 8, 1037−1047

(red line) provide slightly broader IR bands (due to increased thermal motions of the water molecules in the bulk layers), with one main peak located at ~3280 cm^{-1} and a long tail grossly extending to 3000 cm^{-1}, which somehow seems reminiscent of the 3160 cm^{-1} band observed for the interfacial waters but with a much lower amplitude.

The first striking feature is that the two peaks of the interfacial water are almost located at the same position as the peaks of pure liquid water (3350 cm^{-1}, violet line) and pure ice (3200 cm^{-1}, orange line), respectively. Furthermore, using the VDOS decomposition we can immediately assign the ice-like peak of the spectrum to the water molecules accepting a H-bond from out-of-plane silanols (defined before as the ice-like waters), as these water molecules are the only ones contributing to this final active vibrational band. In other words, the 3160 cm^{-1} lower frequency peak arises from the water molecules "strongly H-bonded" to the surface silanols (short H-bond distance of 1.64 Å). Similarly, the liquid-like peak of the spectrum is due to the water molecules donating a H-bond to in-plane silanols (liquid-like waters as previously defined). Therefore, the 3300 cm^{-1} IR band arises from the water molecules "weakly H-bonded" to the surface silanols (long H-bond distance of 1.82 Å). The water molecules "weakly H-bonded" to the surface silanols provide a blue-shifted IR band with respect to the "strongly H-bonded" waters. We also observe an intermediate frequency region in the VDOS between the two main peaks (3160−3300 cm^{-1}), where water molecules assigned as strongly H-bonded (respectively weakly H-bonded) to the surface both contribute to the vibrational signatures. Such intermediate vibrational signatures arise from thermal fluctuations at finite temperature: Dynamics and fluctuations at room temperature will indeed weaken or strengthen the H-bonds formed, thus leading to down- or up-shifts of the vibrational bands. In any case, these intermediate vibrational signatures do not significantly contribute to any IR activity, as there is no specific active IR peak in this region.

The other pivotal information provided by the simulations is that the interfacial water molecules alone already give rise to the two active IR bands and that these two water populations at the direct interface with the surface are enough to provide these two vibrational peaks. As can be seen from Figure 7, the subsequent layers of water mainly contribute to the 3300 cm^{-1} IR band, which indeed is to be expected considering that these water molecules display similar covalent and H-bond lengths as the interfacial liquid-like water molecules. The present spectroscopic modeling thus tends to refute one of the debated SFG assignments of the literature[4,50] which attributes the two peaks to waters belonging to different layers above the surface, supporting instead Shen's interpretations[47] that the liquid- and ice-like vibrational bands come from the interfacial water molecules directly forming different kinds of H-bonds with the quartz surface. It is obvious though that these second layers contribution to the liquid-like peak is intertwined with the first layer adsorbed liquid-like water, so that their participation to the final liquid-like peak can not be completely ruled out. Conversely, they do not contribute to the ice-like peak, which is in turn solely due to the first adsorbed layer of ice-like water molecules.

We would like to comment on the values of the positions of the bands obtained in the present simulations. The present calculations are based on the BLYP functional, which has been successfully applied in the domain of DFT-based ab initio MD simulations of liquids throughout the past decade and is known to provide good to excellent agreements with experiments on structures, dynamics, and spectroscopic properties for instance.[62] In particular, H-bonds in liquids are well reproduced, even without the introduction of dispersion interactions (although usually under an artificially slightly higher temperature of the liquid in the simulation,[63] as done in the present work). The band positions obtained here for pure liquid water and ice are in excellent agreement with the most recent experiments, which once more validates the methodology.

The linear IR bands calculated here for the interfacial water molecules and the silanols at the surface can not be directly compared to the SFG signal. Within the linear response theory, the SFG signal is indeed based on the Fourier transform of the time correlation of the product of the molecular dipole and polarizability,[60] and we have only calculated here the Fourier transform of the time correlation of the molecular dipole moment (which is only part of the SFG signal). We however anticipate that the IR signal calculated here already contains most of the features of the final SFG signal which involves both the IR and Raman activities of the molecules. The difference in the final SFG signal and our calculated IR signal might still be responsible for the slight shifts in position of the peaks between our calculation (3300 and 3160 cm^{-1}) and the true signal in the experiment (3400 and 3200 cm^{-1}). Obviously, our choice of the BLYP functional representation might be responsible by itself for such vibrational shifts. The inclusion of the full SFG spectroscopic signal in the modeling would certainly lead to slight modifications and improvements of the position of the present calculated bands.

Surface Acidity and PZC. Here we turn to the surface acidity calculation and discuss it in relation to the solvation structure of the surface groups and to the vibrational signatures. An accurate description of the solvent behavior is a crucial point in every attempt to characterize the surface acidity. The solvation structure is naturally obtained in MD simulation where an explicit solvent is included. In particular the gradient corrected functionals in DFTMD are well-known to give a very accurate description of the solvation properties of diverse chemical groups. Model systems used in the present work for pK_a calculations are schematically presented in Figure 8, and all

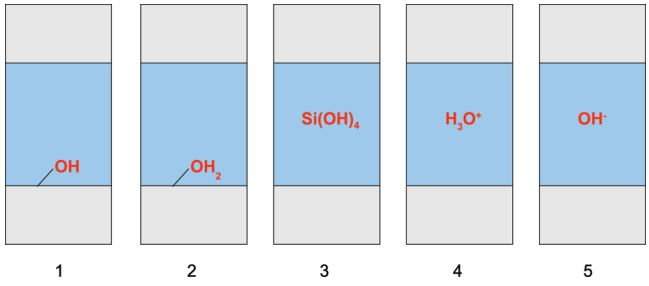

Figure 8. Model systems used for the calculation of pK_a values. For each system the protonated and deprotonated forms are explicitely indicated using the same names as in Table 1 (this text), Table 1 (Supporting Information), and within the text. (1) Silanols on the surface: $-SiOH/-SiOH_d^-$; (2) protonated silanols on the surface: $-SiOH_2^+/-SiOHH_d$; 3) silicic acid: $Si(OH)_4/ Si(OH)_3H_d^-$; (4) solvated excess proton (hydronium): H_3O^+/ H_2OH_d; and (5) localized hydroxide: H_2O/OHH_d^-.

pK_a values are presented in Table 1. The statistical error associated to each pK_a value extracted from the simulations has been calculated as the sum of the statistical error on the deprotonation energy of each group and on the deprotonation

Table 1. pK_a Calculations: Average Vertical Deprotonation Gap ΔE for the Protonated (AH), Deprotonated (A^-), and Middle Point (0.5) States along with the Corresponding Variance σ [a]

compound	ΔE_{AH}	σ_{AH}	ΔE_{A-}	σ_{A-}	$\Delta E_{0.5}$	$\sigma_{0.5}$	ΔA	pK_a	λ
−Si−OH (1)	21.20	0.29	14.64	1.51	19.57	0.31	19.02	8.5 ± 0.6	2.18
−Si−OH (2)	21.07	0.30	15.68	1.19	19.09	0.32	18.85	5.6 ± 0.6	2.22
−Si−OH (1) S2	21.13	0.31	–	–	–	–	–	–	–
−Si−OH (2) S2	20.98	0.30	–	–	–	–	–	–	–
$-Si-OH_2^+$	20.11	0.27	16.13	0.59	18.27	0.34	18.22	−5.0 ± 0.8	1.89
$Si(OH)_4$	21.27	0.29	15.69	1.21	19.35	0.36	19.06	9.2 ± 0.5	2.21
H_3O^+	20.64	0.32	14.97	1.13	18.59	0.43	18.33		2.31
H_2O	21.77	0.29	16.12	0.89	19.67	0.37	19.43	15.4 ± 0.6	2.34

[a]Energies are in eV. In the case of $Si(OH)_4$ the value given for ΔE_{AH} is the average over the deprotonation vertical energies for the four equivalent protons. In the case of H_3O^+ and H_2O the average is over the three and two equivalent protons. Also listed are the deprotonation free energy ΔA calculated with the three-point formula and the corresponding pKa values. The error associated with each pKa calculation is obtained as the sum of the error on the deprotonation free energy calculation of each group (silanol, doubly protonated silanol, etc.) and of the error on the free energy calculation of deprotonation for the hydronium. Statistical errors associated with deprotonation integrals are evaluated as the semi-difference between the value using the first half or the second half of the trajectory only. Details of the methodology can be found in the Supporting Information and is also detailed in our previous works.[28−33] In the last column, the reorganization free energy λ ($\lambda = \Delta E_{AH} - \Delta A$) is reported. The numbers (1) and (2) refer to two different silanol groups, namely the −SiOH forming an in-plane H-bond with a nearby silanol and the out-of-plane −SiOH forming H-bonds with water molecules, respectively. See text for more explanations.

energy of the hydronium. For each deprotonation free energy, the error is calculated as the semidifference between the value from the first and second half of the trajectory. As shown in Table 1, such computational errors are of the order of 0.5−1.0 pH unit. Note however that this does not reflect any error possibly arising from the choice of the DFT functional used in the simulations. Supplementary errors may arise from the numerical quadrature used for the free energy calculation (eq 5 in the Supporting Information), quantum corrections, and finite size effects. This has been discussed in ref 32.

The first quantity of interest is the PZC of quartz which is directly comparable to the experiments. It is calculated from pK_a values for the −SiOH and $-SiOH_2^+$ groups (models 1 and 2 in Figure 8), which determine the possible protonation states of the surface for different values of pH. The calculated value for pK_a of the $-SiOH_2^+$ groups is −5.0. As discussed in the previous paragraph, we can distinguish two types of neutral silanols at the surface of quartz, namely out-of-plane and in-plane. The out-of-plane silanols are the most acidic with a calculated pK_a value of 5.6, while the in-plane silanols are about 3 pK_a units less acidic with a pK_a = 8.5. We thus find a bimodal behavior of the hydroxyls at the silica surface, which is compatible with previous experimental estimates,[47,64]even though the difference we find between the two types of silanols is somewhat smaller than the experimental estimation (anyway within error bars of both calculations and experiments). Note also that our acidic site (pK_a = 5.6) is not as acidic as inferred from experiments (pK_a = 4.5). The lower pK_a of the out-of-plane silanols with respect to the in-plane silanols is in agreement with the results of ref 42 that intermolecular H-bonds on the surface can lower acidity. Moreover, the 'not-so-low' value of the out-of-plane silanols' is also very much compatible with the observation in ref 42 that very acidic groups could only be found on highly strained surface groups. Combining the results for the different groups yields a PZC of 1.0, which is quite close with the experimental value reported for silica and quartz[65] (2−4) and with the value of 1.9 calculated with the MUSIC model in ref 18.

The values of pK_a for both neutral and charged groups have been calculated using the methods that we have recently developed and successfully tested on a series of simple aqueous compounds[28−30,32,33] and for titania surface in contact with water.[31] Using the thermodynamic integration approach, the acid proton in the OH group is gradually removed and transferred to the gas phase. Half reactions for the −SiOH, $-SiOH_2^+$ deprotonation are then combined with the solvation free energy of the proton calculated from the deprotonation free energy of a model hydronium placed among the quartz slabs. Details on the methods can be found in the Supporting Information.

The same methodology is applied to the aqueous silicic acid molecule $Si(OH)_4$ (model 3 in Figure 8). This is a relevant calculation as pK_a values of acid monomers are used as reference in the empirical models for calculations of acidity constants. A pK_a = 9.2 (average over the 4 equivalent OH groups) is found, thus 3 pK_a units more basic than the out-of-plane surface silanols. Such a result is consistent with the anomalous behavior reported in the literature[25] of silica surface being more acid than the corresponding aqueous monomer.

Out-of-plane silanol groups are almost equally accessible to the solvent as the hydroxyl groups of silicic acid and behave very similarly toward H-bonding with the solvent. However subtle differences in the H-bonds and in the internal covalent bonds exist, which can explain the final difference in the pK_a values. Out-of-plane silanols donate a H-bond to water as well as the OH groups of silicic acid do, while the in-plane silanols accept 1.2 H-bonds from water, which is somewhat lower than the 1.4 H-bonds accepted by the OH groups in silicic acid. If we look at the OH_w rdfs (Figure 9), we can notice that if the position of the maxima is very similar for silanols and silicic acid, the H-bond strength is different (estimated as the ratio between the rdf amplitudes at the first peak and subsequent minimum). This indicator seems to point to a stronger H-bond donated and accepted by silicic acid than that donated and accepted by silanols.

Another parameter of the empirical models for acidity constants is the coordination number of the corresponding bases. In such models coordination numbers for depronotated groups are included as a parameter justified a posteriori by the agreement with the experimental data. That is indeed the case for silica, where a higher coordination number with respect to other oxides is used to account for the "anomalous behavior" of

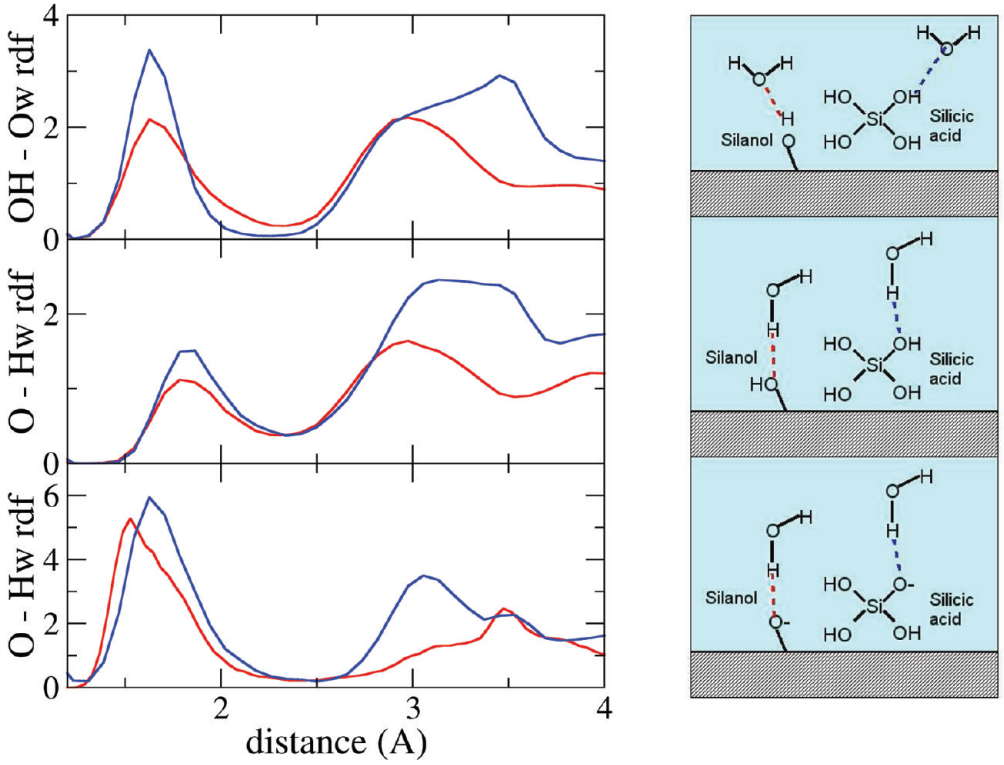

Figure 9. Radial distribution functions for the OH groups at the surface (silanols) and in silicic acid. In the upper panel the H−O_w rdf (donated H-bond) is reported, while in the middle panel the O−H_w rdf (accepted H-bond) is reported for the neutral silanol on the surface and for the neutral silicic acid. In the bottom panel, on the other hand, the O−H_w rdf (accepted H-bond) is reported for the deprotonated silanol on the surface and for the deprotonated silicic acid. Red and blue are used for silanols and silicic acid rdfs, respectively. For more clarity on the right-hand side, the H-bonds which are sampled by the rdfs are also reported as a sketch and are highlighted in red for silanols and blue for silicic acid, respectively.

silica, whose surface pK_a differs from the monomer acid for more than a pK_a unit. Coordination numbers can be directly extracted from the DFTMD. The overall coordination number for the neutral silanols is n_{HB} = 2.2, which includes both H-bonds from water and from the nearby silanols. The DFTMD coordination number is thus lower than the 3 H-bonds chosen for the MUSIC calculations of the acidity of $-SiOH_2^+$ in ref 18. On the other hand, the number of H-bonds extracted from the simulation of the base $-SiO^-$ is 3, exactly as the one chosen for the MUSIC calculations of −SiOH pK_a. Inserting the DFTMD coordination numbers into the MUSIC model[18] and following the strategy of Machesky[66] and our previous investigation,[31] the acidity of $-SiOH_2^+$ predicted by the MUSIC model would be −0.8 instead of −4, raising the PZC from 1.9 to 3.5. Although the shift in the pK_a value is substantial, this does not change the qualitative picture of the silica surface acidity. This is in contrast to our previous experience with the titania surface,[31] where the same strategy reversed the order of the acidity of the two different groups contributing to the PZC. We would also like to comment here that in the specific case of quartz, the MUSIC model encounters the additional difficulty of describing a bimodal behavior of silica. Indeed with the MUSIC approach only a single type of silanol is described, while we have shown that in-plane and out-of-plane silanols can differ by about 3 pH units in their relative acidity.

Combining the information from the solvent organization at the interface, acidity constants of the surface and vibrational bands of the water at the interface, we are able to draw the following conclusions: The local chemistry of the water is modulated by the acidity of groups on the surface. Out-of-plane silanols O−H groups are stronger acids than water O−H groups (respective pK_a's of 5.6 and 15.4, see Table 1) and therefore strongly donate and share their proton into the H-bond network with the water molecules. As a result, the (Si)O−H···O_w H-bond average is 1.64 Å with a (Si)O−H bond length of 1.003 Å and a O_w−H_w of 0.996 Å, to be compared with the O_w−H_w···O_w H-bond of 1.81 Å and O_w−H_w bond length of 0.990 Å in liquid water or to the O_w−H_w···O_w H-bond of 1.76 Å and O_w−H_w bond length of 0.999 Å in ice. As a consequence, the O−H stretching vibration of pure liquid water (3350 cm^{-1}) is red-shifted toward 3160 cm^{-1} and reaches the value of ice (3200 cm^{-1}). This gives rise to the spectroscopically identified "strong H-bond" O−H peak associated with ice-like water molecules, i.e., strongly H-bonded to the silanols surface acid groups. On the other hand, the water molecules that are not strongly bound to the surface experience a very similar situation to that of pure liquid water (for both their H-bond to the surface and for their internal bond lengths), thus leading to the liquid-like band in the vibrational spectrum. Consequently, the associated interfacial IR peak (3300 cm^{-1}) is located very close to the pure liquid water (3350 cm^{-1}). Red shifts depending on the strength of the H-bond network and on the acidity of the neighboring species are well-known in vibrational spectroscopy, even though a quantitative prediction is a difficult task. From our simulations, we have shown that for the interfacial water, when a donated H-bond from a water molecule is replaced by a donated H-bond from a more acid molecule, such as the silanol surface group, the O−H stretch is red-shifted by 200 cm^{-1} . Similar effects would be expected for other oxide surfaces, but the

dx.doi.org/10.1021/ct2007154 | J. Chem. Theory Comput. 2012, 8, 1037−1047

amount of red-shift will depend on the acidity of the surface groups.

Effect of Confinement. Drastic changes can take place in the structure of a fluid when it is confined to spaces of molecular dimensions, as compared to its bulk counterpart. As already emphasized, the understanding of interfacial or confined water at the molecular level is still limited, and the present DFTMD simulations contribute to improve this understanding. The geometry of water confined between the two silica layers could in principle lead to finite size effects on the description of the water solvation, especially in the direction perpendicular to the surface. Things are even more complicated here by the rather small sample of the solid−liquid interface, as a compromise to computational efficiency. Several quantities calculated from the present trajectories give indication that the confinement slightly affects the solvent liquid water properties. As illustration for our discussion, Figure 10 reports the $O_w\cdots H_w$

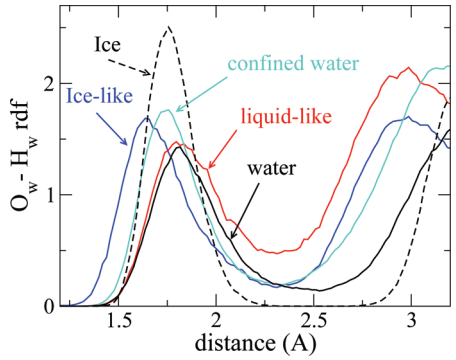

Figure 10. $O_w\cdots H_w$ intermolecular rdfs of pure liquid water (black) and ice (black, dashed) and the confined water layers defined as the two water layers not adsorbed at the quartz surface (cyan), and the identified liquid-like (red) and ice-like (blue) water molecules H-bonded to the surface silanol groups.

rdfs of pure liquid water, ice, the confined water layers defined as the two water layers not adsorbed at the quartz surface and the identified liquid- and ice-like water molecules H-bonded to the surface silanol groups. As already shown in this work, the liquid-like adsorbed molecules give rise to a first rdf peak positioned as in pure liquid water, while the ice-like adsorbed waters display shorter H-bonds than the pure ice counterpart. Interestingly, the rdf of liquid- and ice-like waters display nonzero amplitudes of the minimum, in line with pure liquid water, which is a signature of nonfrozen collective behaviors, contrary to ice. The water molecules that belong to the two solvent layers of the sample which are not adsorbed at the quartz surface give rise to a rdf first peak position identical to ice, while the amplitude of the minimum is again identical to pure liquid water. These confined waters are thus structurally intermediate between the adsorbed liquid- and ice-like water molecules, where the confinement induces shorter H-bonding network than in bulk liquid.

As a consequence, one could expect an increase of the dipole moment of the confined molecules. This is not observed here, and we find that the average dipole moment of the water molecules is 3.1 D, identical in all layers between the two surfaces, also identical for the adsorbed water layers. This value is just in-between pure liquid water (2.9 D) and ice (3.3 D). Vibrational spectroscopy may be the most sensitive property indicating subtle structural changes upon confinement. We have already commented that the IR spectra of the two water layers in-between the quartz surfaces (excluding the adsorbed layers) show a ∼60 cm^{-1} red-shift of the position of the absorption peak with respect to the peak of pure liquid water but still located ∼70 cm^{-1} on the blue side of the ice absorption peak. The broadness of the IR band of the confined waters is comparable to the one of pure liquid water, confirming similar thermal motion of the molecules. The observed red-shift is due to the shorter H-bond network formed by the confined water in comparison to liquid water. Interestingly, even though the rdf first peak of the confined water is identical to ice, the mean covalent O_w-H_w bond length of these molecules is 0.993 Å, closer to pure liquid than ice. This explains why the IR band of the confined water is red-shifted with respect to liquid water (0.993 versus 0.990 Å) but not to the extend of being as shifted as in ice (where the mean covalent bond length is 0.999 Å). Overall, the confined water layers thus behave sufficiently close to liquid water.

In order to further support the use of our hydronium model as reference to calculate the proton solvation free energy, we also calculated the water deprotonation to hydroxide anion. Calculations are carried out within the same setup (model 5 in Figure 8), thus enabling to calculate the water dissociation constant in the confined environment. The value of 15.1 we found for the water dissociation constant is in very good agreement with the experimental value for bulk water.

Another issue could be raised about the effect of the confinement on the solvation structure of the excess proton and on the water acidity properties calculated here. Therefore, we have repeated the calculation of the pK_a of the out-of-plane −SiOH using a larger supercell, where the z cell parameter is increased by about 10 Å. Also, we considered here a full reaction scheme where one silanol group is deprotonated and an excess proton is added to the solution. The pK_a value in the new setup is the same for the half-reaction setup discussed here. Computational details on this additional calculation can be found in the Supporting Information.

The conclusion from that part of the work is that even though there is a strongly adsorbed water layer on each silica surface, the waters in between these two layers exhibit a bulk-like behavior at least in terms of water dissociation constant, structural organization, dipole moments, and spectroscopy. More severe effects of confinement might be expected in the case of silicic acid, which is a bulkier compound compared to the hydronium. However the pK_a value for $Si(OH)_4$ in the water layers is very close to experiment (9.2 versus 9.84), giving us confidence that even this small sample of water layers is capturing the main features of solvation that are responsible for acidity. Note that in order to minimize the effect of the confined geometry, we calculated the deprotonation energies as averages over equivalent protons. However, the difference between equivalent protons is rather small and within 0.1 eV.

SUMMARY AND PERSPECTIVE

DFTMD first-principle MD have been applied to the challenging interrogations of the acidity of the neutral hydroxilated (0001) α-quartz surface and to the spectroscopy of water at the quartz−water interface. We have shown that our theoretical methodology gives a pK_a value of 5.6 for the more acidic out-of-plane silanols and 8.5 for the less acidic in-plane silanols, confirming a bimodal bahavior of the silanols at the (0001) surface. We also find a value of 1.0 for the PZC of the surface that agrees quite well with the experimental

dx.doi.org/10.1021/ct2007154 | J. Chem. Theory Comput. 2012, 8, 1037−1047

measurements. Beyond the calculation of acidity constants and their agreement with experiments, which gives confidence in the theoretical approach employed, the main result from the simulations is the demonstration and understanding at the atomistic level on how the local chemistry of the liquid water is modulated by the acidity of the groups at the surface and vice versa. Indeed, if water influences the surface behavior and is responsible for its acidity, the surface silanols are able in turn to influence and modulate the water properties.

We have shown that the surface out-of-plane silanol O−H groups are stronger acids than O−H water groups from the liquid phase (respective pK_a's of 5.6 and 15.4), and therefore they form strong H-bonds with the water molecules adsorbed at the interface. As a result, the internal geometry of these water molecules as well as their intermolecular H-bond network are closer to those encountered in the ice phase than to those in the liquid phase. Such strong surface water H-bonds ultimately give rise to a 200 cm^{-1} red-shift of the O−H stretching motion of the adsorbed water with respect to the value of pure liquid water. This local strong H-bond network is therefore responsible for the 3160 cm^{-1} vibrational band observed in nonlinear VSFG experiments and identified as the ice-like band because of the internal O−H and intermolecular H-bond O−H···O network properties which are close to those encountered in ice.

We have also identified a second population of water molecules adsorbed at the quartz surface, acting as H-bond donors that are not so strongly bound to the surface. They have properties close to those of pure liquid water, i.e., for intra- and intermolecular distances, and are responsible for the liquid-like O−H band in the VSFG spectrum. This peak is consequently located as in pure liquid water (3350 cm^{-1}). Such ice- and liquid-like terms are borrowed from the language of vibrational spectroscopy and refer, as demonstrated here, to two populations of water molecules adsorbed as a first layer at the hydroxylated quartz surface, i.e., one population strongly H-bonded to the surface and one population weakly H-bonded to the surface. We have also shown that this simple interpretation is slightly complicated by thermal fluctuations and the associated dynamical behavior of the H-bonds.

The present investigation serves as a link between the macroscopic acidity property of a surface and the molecular structure of the liquid at the interface, ultimately giving an understanding of the interfacial vibrational spectroscopy in terms of the local chemistry that occurs at the surface water interface. The molecular approach employed here has allowed to identify the more acidic sites at the surface, using the link between acidity and vibration. The present investigation was centered on quartz, similar effects are expected for other oxide surfaces, but the amount of red-shift will depend on the acidity of the surface groups. Our approach is expected to be especially valuable for those cases where there are more nonequivalent acidic sites on the surface and where the experimental measure would not permit to distinguish between them.

The key is the identification of the local arrangement at the interface relating sites acidity, surface water, and water−water H-bond networks and interfacial water vibrational spectroscopy. Such methodology is currently applied to several oxide surfaces in order to provide a molecular comprehensive understanding of surface acidity.

METHODS

DFT-based Born−Oppenheimer MD (BO MD) simulations were performed using the Becke exchange[67] and Lee−Yang−Parr[68] correlation functionals. All the calculations have been carried out with the freely available DFT package CP2K/Quickstep,[69] which is based on the hybrid Gaussian and plane wave method.[70] Analytic Goedecker−Teter−Hutter[71,72] pseudopotentials, a TZV2P level basis set for the orbitals, and a density cutoff of 280 Ry were used. Only the Γ point was considered. The simulations have been performed in the NVT ensemble with a Nose thermostat and a target temperature of 330 K.

The acidity constants of surface silanols and silicic acid are computed using the reversible proton insertion/deletion method that we have recently developed and successfully tested on a series of simple aqueous compounds.[28,29,32] The IR spectra are calculated from the Fourier transform of the dipole time correlation function,[73] as described in our previous works.[61,62,74−78] The total dipole moment of the system (sum of ionic and electronic contributions,[79]) is calculated using the modern theory of polarization framework,[80,81] developed by Silvestrelli and Parrinello.[79,82,83] The separation into individual molecular contributions is performed within the localized Wannier orbitals, as implemented within the CPMD package.[84,85] More details on the protocols applied in the present investigation are available in the Supporting Information.

ASSOCIATED CONTENT

Supporting Information

Model systems, method for acidity constant calculations, and more details on spectroscopy. This material is available free of charge via the Internet at http://pubs.acs.org.

AUTHOR INFORMATION

Corresponding Author

*E-mail: mgaigeot@univ-evry.fr.

Notes

The authors declare no competing financial interest.

ACKNOWLEDGMENTS

M.S. is grateful to EPSRC for financial support. This work was granted access to the HPC resources of IDRIS under the allocation 2009-2010[0712484] made by Grand Equipement National de Calcul Intensif (GENCI) in France. Part of the calculations have been performed using an allocation of computer time on HECToR, the U.K.'s high-end computing resource, as part of the a grant to the UKCP consortium. M.P.G acknowledges the Churchill College in Cambridge, U.K. and the French Foreign Office for the allowance of an Overseas Fellowship, and the PHC Partenariat Hubert Curien - Alliance Program for further financial support.

REFERENCES

(1) Diebold, U. *Nat. Mater.* **2010**, *9*, 185.
(2) Enterkin, J. A.; Subramanian, A. K.; Russell, B. C.; Castell, M. R.; Poeppelmeier, K. R.; Marks, L. D. *Nat. Mater.* **2010**, *9*, 245.
(3) He, Y.; Tilocca, A.; Dulub, O.; Selloni, A.; Diebold, U. *Nat. Mater.* **2009**, *8*, 585.
(4) Maccarini, M. *Biointerphases* **2007**, *2*, MR1.
(5) Ohlin, C. A.; Villa, E. M.; Rustad, J. R.; Casey, W. H. *Nat. Mater.* **2010**, *9*, 11.
(6) Casey, W. H.; Ludwig, C. *Nature* **1996**, *381*, 506.
(7) Ball, P. *Chem. Rev.* **2008**, *108*, 74.

(8) Ball, P. *Nature* **2008**, *452*, 291.
(9) Hodgson, A.; Haq, S. *Surf. Sci. Rep.* **2009**, *64*, 381.
(10) Michaelides, A.; Morgenstern, K. *Nat. Mater.* **2007**, *6*, 597.
(11) Wandelt, K.; Thurgate, S. *Solid-Liquid Interfaces: Macroscopic phenomena - Microscopic understanding*; Springer-Verlag: Berlin, Germany, 2003.
(12) Jena, K. C.; Hore, D. K. *J. Phys. Chem. C* **2009**, *113*, 15364.
(13) Nilsson, A.; Pettersson, L. G. M.; Norskov, J. K. *Chemical bonding at surfaces and interfaces*; Elsevier: Oxford, U.K., 2008.
(14) Grassian, V. H. *Environmental catalysis*; Taylor and Francis: Boca Raton, FL, 2005.
(15) Hazen, R. M.; Sverjensky, D. A. *Cold Spring Harbor Perspect. Biol.* **2010**, *2*, a002162.
(16) Gray, J. *Curr. Opin. Struct. Biol.* **2004**, *14*, 110.
(17) Somorjai, G.; Frei, H.; Park, J. *J. Am. Chem. Soc.* **2009**, *131*, 16589.
(18) Hiemstra, T.; Vanema, P.; Riemsdijk, W. V. *Colloid Interface Sci.* **1996**, *184*, 680.
(19) Bickmore, B.; Rosso, K.; Nagy, K.; Cygan, R.; Tadanier, C. J. *Clays Clay Miner* **2003**, *51*, 359.
(20) Bickmore, B.; Tadanier, C.; Rosso, K.; Monn, W.; Egget, D. *Geochim. Cosmochim. Acta* **2004**, *68*, 2025.
(21) Sverjensky, D. *Geochim. Cosmochim. Acta* **1994**, *58*, 3123.
(22) Sverjensky, D.; Sahai, N. *Geochim. Cosmochim. Acta* **1996**, *60*, 3773.
(23) Sahai, N. *Geochim. Cosmochim. Acta* **2000**, *64*, 3629.
(24) Hiemstra, T.; Riemsdijk, W. V.; Bolt, G. *J. Colloid Interface Sci.* **1989**, *133*, 91.
(25) Sahai, N. *Environ. Sci. Technol.* **2002**, *36*, 445.
(26) Liptak, M.; Shields, G. *J. Am. Chem. Soc.* **2001**, *123*, 7314.
(27) Saracino, G.; Improta, R.; Barone, V. *Chem. Phys. Lett.* **2003**, *373*, 411.
(28) Sulpizi, M.; Sprik, M. *Phys. Chem. Chem. Phys.* **2008**, *10*, 5238.
(29) Cheng, J.; Sulpizi, M.; Sprik, M. *J. Chem. Phys.* **2009**, *131*, 154504.
(30) Sulpizi, M.; Sprik, M. *J. Phys.: Condens. Matter* **2010**, *22*, 284116.
(31) Cheng, J.; Sprik, M. *J. Chem. Theory Comput.* **2010**, *6*, 880.
(32) Costanzo, F.; Sulpizi, M.; Valle, R.; Sprik, M. *J. Chem. Phys.* **2011**, *134*, 244508.
(33) Mangold, M.; Rolland, L.; Costanzo, F.; Sprik, M.; Sulpizi, M.; Blumberger, J. *J. Chem. Theory Comput.* **2011**, *7*, 1951.
(34) de Leeuw, N.; Higgins, F.; Parker, S. *J. Phys. Chem. B* **1999**, *103*, 1270.
(35) Lu, Z.; Sun, Z.; Li, Z.; An, L. *J. Phys. Chem. B* **2005**, *109*, 5678.
(36) Skelton, A. A.; Fenter, P.; Kubicki, J. D.; Wesolowski, D. J.; Cummings, P. T. *J. Phys. Chem. C* **2011**, *115*, 2076.
(37) Riganese, G.; Vita, A. D.; Charlier, J.; Gonze, X.; Car, R. *Phys. Chem. Chem. Phys.* **2004**, *6*, 1920.
(38) Yang, J.; Meng, S.; Xu, L.; Wang, E. *Phys. Rev. B* **2005**, *71*, 035413.
(39) Yang, J.; Wang, E. *Phys. Rev. B* **2006**, *73*, 035406.
(40) Goumans, T.; Wander, A.; Brown, W.; Catlow, C. *Phys. Chem. Chem. Phys.* **2007**, *9*, 2146.
(41) Adeagbo, W.; Doltsinis, N.; Klevanika, K.; Renner, J. *ChemPhysChem* **2008**, *9*, 994.
(42) Leung, K.; Nielsen, I.; Criscenti, L. *J. Am. Chem. Soc.* **2009**, *131*, 18358.
(43) Shen, Y. R. *Nature* **1989**, *337*, 519.
(44) Du, Q.; Freysz, E.; Shen, Y. R. *Phys. Rev. Lett.* **1994**, *72*, 238.
(45) Du, Q.; Freysz, E.; Shen, Y. R. *Science* **1994**, *264*, 826.
(46) McGuire, J. A.; Shen, Y. R. *Science* **2006**, *313*, 1945.
(47) Ostroverkhov, V.; Waychunas, G. A.; Shen, Y. R. *Phys. Rev. Lett.* **2005**, *94*, 046102.
(48) Zhang, L.; Tian, C.; Waychunas, G. A.; Shen, Y. R. *J. Am. Chem. Soc.* **2008**, *130*, 7686.
(49) Ostroverkhov, V.; Waychunas, G. A.; Shen, Y. R. *Chem. Phys. Lett.* **2004**, *386*, 144.
(50) Gureau, M. C.; Kim, G.; Lim, S. M.; Albertorio, F.; Fleischer, H. C.; Cremer, P. *ChemPhysChem* **2003**, *4*, 1231.
(51) Bertie, J. E.; Labbé, H. J.; Whalley, E. *J. Chem. Phys.* **1969**, *50*, 4501.
(52) Scherer, J. R.; Snyder, R. G. *J. Phys. Chem.* **1977**, *67*, 4794.
(53) Rusk, A. N.; Williams, D.; Querry, M. R. *J. Opt. Soc. Am.* **1971**, *61*, 895.
(54) Afsar, M. N.; Hasted, J. B. *J. Opt. Soc. Am.* **1977**, *67*, 902.
(55) Segelstein, D. The complex Refractive Index of Water; *M.S. Thesis*; University of Missouri: Columbia, MO, 1981.
(56) Buch, V. *J. Phys. Chem. B* **2005**, *109*, 17771.
(57) Eftekhari-Bafrooei, A.; Borguet, E. *J. Am. Chem. Soc.* **2009**, *131*, 12034.
(58) Allen, H. C.; Casillas-Ituarte, N. .; Sierra-Hernandez, M. R.; Chen, X.; Tang, C. Y. *Phys. Chem. Chem. Phys.* **2009**, *11*, 5538.
(59) Richmond, G. L. *Annu. Rev. Phys. Chem.* **2001**, *52*, 357.
(60) Morita, A.; Hynes, J. T. *J. Phys. Chem. B* **2002**, *106*, 673.
(61) Gaigeot, M. P.; Martinez, M.; Vuilleumier, R. *Mol. Phys.* **2007**, *105*, 2857.
(62) Gaigeot, M. P. *Phys. Chem. Chem. Phys.* **2010**, *12*, 3336.
(63) Zhang, C.; Donadio, D.; Gygi, F.; Galli, G. *J. Chem. Theory Comput.* **2011**, *7*, 1443.
(64) Ong, S.; Zhao, X.; Eisenthal, K. B. *Chem. Phys. Lett.* **1992**, *191*, 327.
(65) Kosmulski, M. *J. Colloid Interface Sci.* **2002**, *253*, 77.
(66) Machesky, M.; Predota, M.; Wesolowski, D.; Vlcek, L.; Cummings, P.; Rosenqvist, J.; Ridley, M.; Kubicki, J.; Bandura, A.; Kumar, N.; Sofo, J. *Langmuir* **2008**, *24*, 12331.
(67) Becke, A. *Phys. Rev. A* **1988**, *38*, 3098.
(68) Lee, C.; Yang, W.; Parr, R. G. *Phys. Rev. B* **1988**, *37*, 785−789.
(69) The CP2K developers group; http://cp2k.berlios.de/.
(70) Lippert, G.; Hutter, J.; Parrinello, M. *Mol. Phys.* **1997**, *92*, 477.
(71) Goedecker, S.; Teter, M.; Hutter, J. *Phys. Rev. B* **1996**, *54*, 1703.
(72) Hartwigsen, C.; Goedecker, S.; Hutter, J. *Phys. Rev. B* **1998**, *58*, 3641.
(73) McQuarrie, D. *Statistical Mechanics*; Harper-Collins Publishers: New York, 1976.
(74) Gaigeot, M. P.; Sprik, M. *J. Phys. Chem. B* **2003**, *107*, 10344.
(75) Gaigeot, M. P.; Vuilleumier, R.; Sprik, M.; Borgis, D. *J. Chem. Theory Comput.* **2005**, *1*, 772.
(76) Marinica, C.; Grégoire, G.; Desfrançois, C.; Schermann, J. P.; Borgis, D.; Gaigeot, M. P. *J. Phys. Chem. A* **2006**, *110*, 8802.
(77) Grégoire, G.; Gaigeot, M. P.; Marinica, D. C.; Lemaire, J.; Schermann, J. P.; Desfrançois, C. *Phys. Chem. Chem. Phys.* **2007**, *9*, 3082.
(78) Gaigeot, M. P. *J. Phys. Chem. A* **2008**, *112*, 13507.
(79) Silvestrelli, P.; Bernasconi, M.; Parrinello, M. *Chem. Phys. Lett.* **1997**, *277*, 478.
(80) King-Smith, R.; Vanderbilt, D. *Phys. Rev. B* **1993**, *47*, 1651.
(81) Vanderbilt, D.; King-Smith, R. *Phys. Rev. B* **1993**, *48*, 4442.
(82) Silvestrelli, P.; Parrinello, M. *J. Chem. Phys.* **1999**, *111*, 3572.
(83) Bernasconi, M.; Silvestrelli, P.; Parrinello, M. *Phys. Rev. Lett.* **1998**, *81*, 1235.
(84) Car, R.; Parrinello, M. *Phys. Rev. Lett.* **1985**, *55*, 2471.
(85) Parrinello, M.; Andreoni, W.; Curioni, A. *CPMD*, version 3.7.1; IBM Corporation and Max Planck Institute Stuttgart: Armonk, NY and Stuttgart, Germany.